Available online at www.sciencedirect.com

ScienceDirect

Materials Today: Proceedings 7 (2019) 619–624

materialstoday: PROCEEDINGS

www.materialstoday.com/proceedings

Nanotech Malaysia 2018

A study of stoichiometric composition of Ge thermal oxide by X-ray photoelectron spectroscopic depth profiling

Mohammad Anisuzzaman[a], Norani Ab Manaf[a], Suhairi Saharudin[b], Kanji Yasui[c], Abdul Manaf Hashim[a]*

[a]*Malaysia-Japan International Institute of Technology, Universiti Teknologi Malaysia, Jalan Sultan Yahya Petra, 54100 Kuala Lumpur, Malaysia*

[b]*MIMOS Semiconductor (M) Sdn Bhd, Technology Park Malaysia, 57000 Kuala Lumpur, Malaysia*

[c]*Department of Electrical Engineering, Nagaoka University of Technology, 1603-1 Kamitomioka-machi, Nagaoka, Niigata 940-2188, Japan*

Abstract

The evolution of different oxidation states during thermal oxidation of (100) oriented Ge substrate was investigated with X-ray photoelectron spectroscopic analysis. The thermally grown oxides in the temperature range of 380 to 500^{o}C were found to consist of four different oxidation states of Ge, namely, Ge^{1+}, Ge^{2+}, Ge^{3+}, and Ge^{4+}. The fractional composition of the oxide species is seen to be dependent on oxidation temperature. Spectroscopic depth profiling reveals variation of oxide composition along the depth of the oxide layer with a large concentration of GeO_2 near the oxide surface and a large concentration of suboxides near the oxide/Ge interface. The results obtained in the investigation will help in achieving greater insight into the thermal oxidation process of Ge.

Selection and peer-review under responsibility of the scientific committee of the Nanotech Malaysia 2018.

Keywords: Germanium; thermal oxidation; XPS; suboxide

1. Introduction

Recent advancement in Ge MOSFET technology has demonstrated the potential to substitute Si for next generation microprocessors [1,2]. A critical issue in the maturation of high performance Ge MOSFETs is the

* Corresponding author. Tel.: +603-2202-1517; fax: +603-2203-1266.
E-mail address: abdmanaf@utm.my

Selection and peer-review under responsibility of the scientific committee of the Nanotech Malaysia 2018.

development of a gate-stack with low interface state density (D_{it}) [3,4]. Because of the thermal instability and water solubility of thermally grown Ge-oxide, researchers have previously tried to obtain Ge-MOS gate-stack with high-k dielectrics (e.g. Al_2O_3, HfO_2, ZrO_2, etc.) without satisfactory results mainly due to the poor interface quality between the high-k dielectrics and Ge channel [5,6]. In recent years, research on Ge-MOS gate-stack have shown that Ge surface passivation by its native oxide is essential in achieving high quality interface. Significantly low D_{it} and high field-effect mobility were demonstrated by multilayer passivation with GeO_x as the interfacial layer [7-9]. For surface passivation by GeO_x, the interface quality is highly dependent on Ge oxidation conditions, possibly due to the dependence of oxide stoichiometry and morphology on processing temperatures.

Rapid desorption of germanium monoxide (GeO) from GeO_2 passivation layer along with degradation of interface quality was reported for temperatures above 400^{o}C [10]. Gate Ge oxide grown at 500^{o}C at 0.1 MPa pressure was found to be highly leaky, making C-V measurement impossible [11]. On the other hand, suppression of GeO desorption by high-pressure oxidation at 550^{o}C showed significant improvement in interface quality [11]. It is obvious that a comprehensive understanding of thermal oxidation behavior of Ge is necessary in order to achieve the optimum oxidation conditions for interfacial GeO_x. More specifically, it is necessary to thoroughly investigate the stoichiometric evolution of Ge thermal oxide in a wide oxidation temperature range as the oxide stoichiometry can have important impact on the overall oxide layer quality and D_{it}. We investigated the stoichiometric composition and growth evolution of different oxide species in thermally grown Ge oxide by X-ray photoelectron spectroscopic (XPS) analysis. The stoichiometric variation along the oxide depth was investigated by XPS depth profiling. The results reveal some fundamental aspects of Ge thermal oxide growth process. Comprehensive understanding of the growth behavior by investigating a wide range of growth temperatures, growth times, oxygen (O_2) flow rates, annealing speed and substrate treatment will greatly assist in the achievement of optimum conditions for high-quality interfacial oxide formation.

2. Experimental

Czochralski grown p-type Ge wafers of (100) surface orientation and a resistivity of ~13.25 ohm-cm is used for the oxidation experiments. Particulate and organic contaminations are removed by sonication in acetone, ethanol, and Milli-Q water. Subsequently, the wafers are immersed in 10% HCl solution for 10 min followed by cyclic rinse in 2% HF solution and H_2O with total immersion of 5 min in HF solution to remove natural oxide. The HF treatment leaves a H-passivated surface that prevents immediate regrowth of the oxide. Following the HF treatment, the wafers are quickly loaded into a rapid thermal annealing (RTA) chamber and kept in pure N_2 flow to prevent natural oxide formation. For greater control over the oxidation temperature and time, an ULVAC-RIKO infrared gold image furnace (model SSA-E45P) is used for all the oxidation experiments. Prior to oxidation, the substrates are heat treated at 550^{o}C in pure N_2 to remove any remaining volatile natural oxide of Ge. To maintain precision on the oxidation time, the furnace temperature is quickly ramped up to the desired oxidation temperature while the wafers are kept in pure N_2 flow. As soon as the temperature stabilizes, dry O_2 at a preset flow rate is started and the N_2 flow is adjusted as required. The flow rate of O_2 is fixed at 1.0 l/min. The oxidation is done at the atmospheric pressure since such condition is easily realized and considered as a practical processing pressure. After the oxidation time, the O_2 flow and infrared lamps are turned off and the N_2 flow is increased. The furnace is allowed to cool down naturally. A range of oxidation temperatures (380 to 500^{o}C) and duration (2 to 20 min) are investigated to obtain a comprehensive understanding of the oxide growth process. X-ray photoelectron spectroscopic measurements of the as-grown oxide layers were performed by a ULVAC-Phi Quanterra II XPS system with Al *kα* source (1486.6 eV). The analyzer take off angle is set at 45^o and the scan resolution is set at 0.1 eV for all samples. To obtain accurate composition of oxide species, XPS depth profiling is performed in which the oxide is removed layer by layer using Ar-ion sputtering in multiple cycles and XPS scan performed in each cycle until only elemental Ge signal is detected.

3. Results and discussion

For accurate study of thermal oxide growth behavior, it is necessary to ensure complete removal of natural oxide from the substrate surface. To verify the effectiveness of natural oxide removal by the cleaning process, the Ge 3*d*

core level photoelectron spectra from the substrate before and after HF treatment are obtained, as shown in Fig. 1(a) and 1(b), respectively. The Ge elemental peak is centered around the binding energy of 29.4 eV. A strong oxide peak to the left of the elemental Ge peak is seen in the non-treated substrate, while the oxide peak is completely removed in the HF-treated substrate. The HF-treated substrate was kept in a vacuum desiccator for 24 hours before obtaining the spectra. When the HF treated substrate was kept exposed to clean room air for 24 hours, photoelectron spectrum shows the appearance of a small oxide peak as shown in Fig. 1(c). Therefore, although the HF treatment effectively removes the natural oxide from the Ge substrate surface, the passivation is not effective in preventing oxide formation in substrates exposed to the air for extended duration.

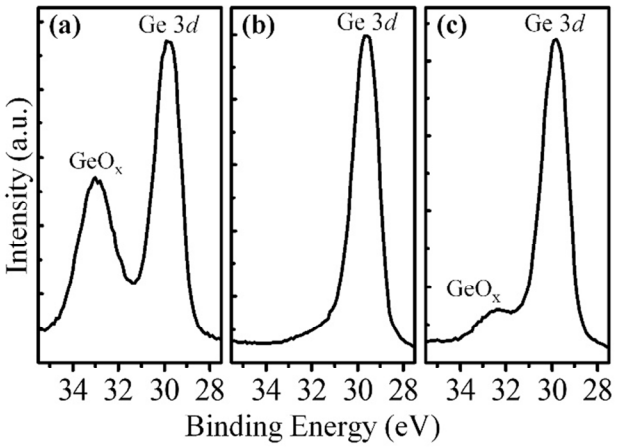

Fig. 1. X-ray photoelectron spectra from Ge substrate (a) before HF-treatment, (b) after HF-treatment, and (c) after 24 hr air exposure following HF-treatment.

In order to get an accurate picture of the evolution of the different oxidation states during thermal oxidation of Ge, substrates are oxidized at 380°C for durations ranging from 2 to 20 min in 1.0 *l*/min O_2 flow. The lower temperature ensures the minimization of desorption induced change of oxide composition of the as-grown oxide layers. The Ge 3*d* photoelectron spectra obtained from surfaces of oxidized substrates are shown in Fig. 2(a), (b) and (c) for oxidation durations of 2, 5 and 10 min, respectively. To find out the stoichiometric composition, the spectral envelope is deconvoluted into peak functions consisting of the Ge elemental components and oxidation state components by fitting. To fit the envelope spectrum, first of all, the baseline originating from scattered photoelectrons is removed by a Shirley-type function. The Ge 3*d* elemental peak envelope centered at 29.4 eV binding energy is fitted by the two Voigt functions (convoluted Gaussian-Lorentzian or G-L functions) representing the peaks originating from Ge $3d_{5/2}$ and Ge $3d_{3/2}$ split-spin orbits and appear at an energy separation ΔE = 0.59 eV and an area ratio of (2*5/2+1):(2*3/2+1) = 1:0.67. The FWHM of these peaks are determined to be 0.99±0.04 eV from an Ar-ion sputter cleaned Ge substrate. In addition, a small intensity component about 1.5 eV below the Ge $3d_{5/2}$ core level peak is used to obtain proper fit for the Ge elemental spectrum. This peak is assumed to envelop oxide-related component and surface dimer component [12,13].

Reports on Ge oxide analysis by synchrotron radiation photoelectron spectroscopy have revealed four distinct oxidation states of Ge, namely Ge^{1+}, Ge^{2+}, Ge^{3+}, and Ge^{4+} corresponding to the oxides Ge_2O, GeO, Ge_2O_3, and GeO_2, respectively [12,14]. Each of the oxidation states correspond to a chemical shift of approximately 0.85 eV (due to each O-bond) from the Ge elemental peak. We obtained satisfactory fit by placing Voigt functions at ΔE of 0.85±0.05 eV for Ge^{1+}, 1.7±0.1 eV for Ge^{2+}, 2.5±0.1 eV for Ge^{3+}, and 3.4±0.2 eV for Ge^{4+} from the Ge $3d_{5/2}$ core level peak. Some peak shifts were observed that may have resulted from positive charging of the oxide layer due to electron depletion and also due to band bending owing to the more electronegative O in the Ge-O compound [15]. The FWHM of the function corresponding to Ge^{4+} oxidation state was strictly constrained at 1.65±0.05 eV. This was obtained from a thick oxide layer where a single peak at the GeO_2 binding energy position fitted the spectrum. The

FWHM of Ge^{2+} and Ge^{3+} oxidation state peaks were found from best fit and constrained at 1.3±0.1 eV while the Ge^{1+} state was set at 1.1±0.1 eV for all fitting peaks functions. The deconvoluted spectra reveal that a thin oxide layer appears after 2 min oxidation consisting of all four oxidation states as can be seen in Fig. 2(a). Area analysis of the peaks show that about 47% of the oxide layer is GeO_2. An enhanced growth of GeO_2 is observed after 5 min oxidation as indicated by the significant increase in Ge^{4+} peak intensity in Fig. 2(b), reaching 69.7% concentration. Further increase of the Ge^{4+} peak intensity occurs after 10 min of oxidation (Fig. 2(c)) where GeO_2 concentration reaches 78.6%. However, increasing the oxidation time to 20 min shows almost no change in oxide peak intensity. This possibly indicates a limit to the oxide thickness achievable at 380°C.

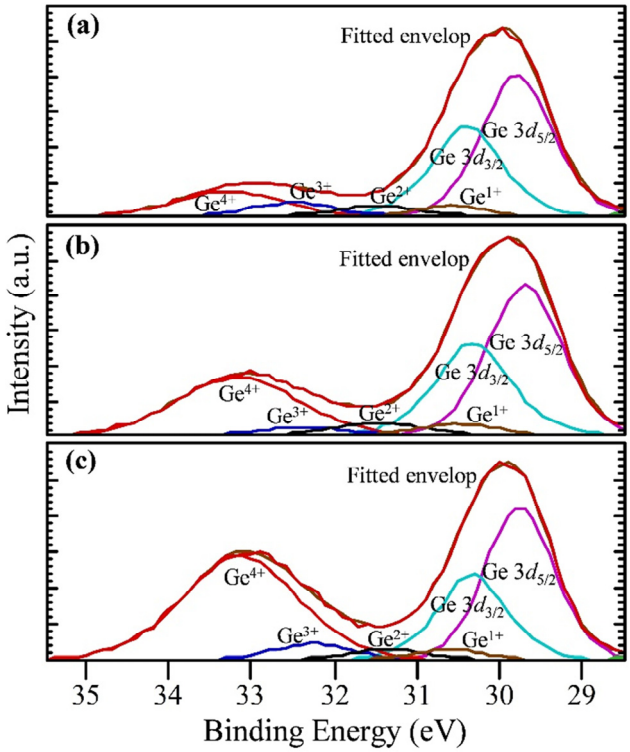

Fig. 2. Deconvoluted X-ray photoelectron spectra from Ge substrate oxidized at 380°C in dry O_2 for (a) 2 min, (b) 5 min, and (c) 10 min.

From surface photoelectron spectra of oxide formed at 380°C, it appears that the oxide thickness increases mostly with the enhanced growth of GeO_2. However, the continued appearance of suboxide peaks in the spectra raises concern about the stoichiometric composition near the oxide/Ge interface. To find out if there is variation of oxide composition along the depth of the oxide layer, XPS depth profiling was performed on two samples oxidized at 400°C (10 min) and 500°C (1 min). It is noted here that the depth profiling of sample 380°C was not done because the thickness of Ge oxide layer is too thin, and the roughness is also high. The Ge 3*d* photoelectron spectra of these samples are shown in Fig. 3(a) and (b) where the spectrum 0 of the depth profile axis is taken at the oxide surface and the subsequently numbered spectra are taken after removal of a layer of oxide by Ar-ion sputtering in consecutive cycles. Interestingly, from the surface spectrum to subsequent spectra, we see a clear shift of the oxide envelop peak to lower energy. This means there is significant change in oxide composition along the oxide layer depth. To determine the precise variation of oxidation states along the layer depth, spectral deconvolution was performed on the photoelectron spectra obtained from the oxide surface and all the sputter cycles using the same constrains on fitting parameters as mentioned before. Area analysis of the deconvoluted oxide peak functions reveals an interesting picture of the stoichiometric variation in the oxide layer. Fig. 3(c) and (d) presents these variations as percentage concentration of the four oxide species obtained at different sputter cycles. In these figures, the cycle 0

represents the oxide surface and subsequent cycles are along the oxide depth until the oxide/Ge interface is reached. The interface is approximately determined from Ge elemental and oxide peak intensity comparison. The plots show a complex distribution of the oxide components in the thermally grown oxide layer.

In 400°C oxidation, we see in Fig. 3(c) that the GeO_2 concentration at the surface (82.8%) falls off sharply (to 16%) in the first sputter cycle and further drops to 9% near the interface. This indicates a rather thin layer of high concentration GeO_2 at the surface of the oxide. Both Ge_2O_3 and GeO concentration increases sharply to 34.40% and 38.75%, respectively, in the first cycle. However, whereas the GeO concentration remains constant along the depth, the Ge_2O_3 concentration drops off again to about 12% near the interface. The concentration of Ge_2O increases steadily along the depth and approaches that of GeO near the interface. The concentration profile shows that the oxide near the interface is primarily composed of GeO and Ge_2O. Oxidation at 500°C results in some interesting changes in the oxide concentration distribution. In this case, the surface appears to consist entirely of GeO_2 with concentration above 99%, which then falls off almost linearly along the depth of the oxide layer, reaching zero at the interface. The Ge_2O_3 concentration gradually increases along the oxide depth to a peak of 34.6% on cycle 5 and then gradually falls off to zero. The GeO concentration increases almost linearly from the surface till the interface, reaching maximum at the interface (53.7%). The Ge_2O concentration remains insignificant till halfway through the oxide layer, which then gradually increases to the maximum (46.3%) at the interface. The interface region appears to be composed almost entirely of GeO and Ge_2O.

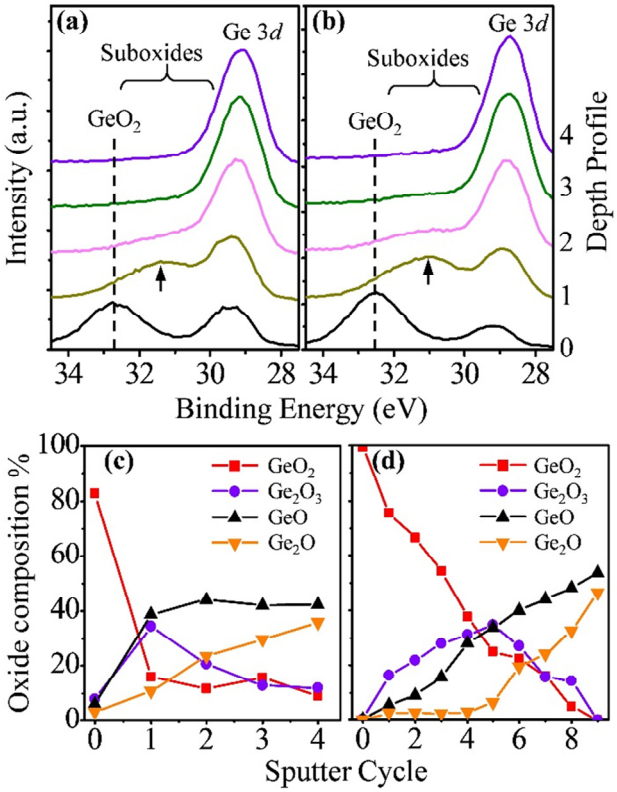

Fig. 3. XPS depth profiles for Ge substrates oxidized at (a) 400°C for 10 min and (b) 500°C for 1 min and the percentage concentration of oxide components along the depth of the oxide layer in (c) 400°C/10 min and (d) 500°C/1 min oxidized samples.

The continuous fall off of GeO_2 concentration along the oxide depth and the abundance of suboxides at the interface reveals a fundamental process in the thermal oxidation of Ge substrate. It appears that thermal oxidation of Ge results in the primary growth of Ge_2O and GeO suboxide species. The primary growth of suboxides has also been observed during thermal oxidation of Ge substrate in atomic O at lower temperatures by Molle et al [16]. We assume that the primarily formed suboxides are further oxidized into Ge_2O_3 and finally GeO_2 at elevated

temperatures. The oxide evolution seems to depend not only on temperature but also on O_2 availability. The permeation of O_2 through the as-formed oxide layer becomes restricted as the oxide thickness increases. Hence, we see the gradient of GeO_2 along the oxide depth. Near the surface, most of the suboxides including Ge_2O_3 are converted to GeO_2, thus the drop in Ge_2O_3 concentration. However, a complete conversion of the suboxides into GeO_2, even with prolonged oxidation time, is prevented likely due to GeO_2 decomposition at the oxide/Ge interface along with continuous desorption and growth of oxides [10]. This result shows that the concentration of GeO_2 is high at higher temperature even with short oxidation time. Here, we can also conclude that the effect of temperature is much more significant as compared to the oxidation time. More study on the effects of desorption on oxide composition is necessary to understand the process.

4. Conclusion

All In conclusion, the study shows some fundamental characteristics of thermal oxidation of (100) oriented Ge substrate in dry O_2. A complex stoichiometric composition of four different oxidation states was found in the oxide layer. Isothermal oxidation at 380^{o}C show the GeO_2 concentration in the oxide layer increases with time. Increasing the oxidation temperature up to 500°C seems to increase the GeO_2 concentration towards 100% at the surface area. However, depth profiling reveals variation of stoichiometric composition along the depth of the oxide layer. Despite the apparent enhancement of GeO_2 at the surface at higher oxidation temperature and time, the interface region is consistently found to be composed mostly of suboxides.

Acknowledgements

M. A. wishes to thank Universiti Teknologi Malaysia for postdoctoral fellowship. N. A. M. thanks MARA and MOE for research scholarship. This work was funded by FRGS, MJIIT, Universiti Teknologi Malaysia, Malaysia Ministry of Science, Technology and Innovation, and the Malaysia Ministry of Education.

References

[1] C.O. Chui, H. Kim, P.C. McIntyre, K.C. Saraswat, IEDM Tech. Dig. (2003) 437.
[2] D. Kuzum, A.J. Pethe, T. Krishnamohan, Y. Oshima, Y. Sun, J.P. McVittie, P.A. Pianetta, P.C. McIntyre, K.C. Saraswat, IEDM Tech. Dig. (2007) 723.
[3] H. Murakami, T. Fujioka, A. Ohta, T. Bando, S. Higashi, S. Miyazaki, ECS Trans. 33 (2010) 253.
[4] A. Ohta, T. Fujioka, H. Murakami, H. Higashi, S. Miyazaki, Jpn. J. Appl. Phys. (2011) 5010PE01.
[5] N. Wu, Q. Zhang, C. Zhu, C.C. Yeo, S.J. Whang, D.S.H. Chan, M.F.Li, B.J. Cho, A. Chin, D.L. Kwong, A.Y. Du, C.H. Tung, N. Balasubramanian, Appl. Phys. Lett. 84 (2004) 3741.
[6] R. Xie, M. Yu, M.Y. Lai, L. Chan, C. Zhu, Appl. Phys. Lett. 92 (2008) 163505.
[7] R. Zhang, T. Iwasaki, N. Taoka, M. Takenaka, S. Takagi. Appl. Phys. Lett. 98 (2011) 112902.
[8] K. Hirayama, K. Yoshino, R. Ueno, Y. Iwamura, H. Yang, D. Wang, H. Nakashima, Solid-State Electron. 60 (2011) 122.
[9] K. Yamamoto, T. Sada, D. Wang, H. Nakashima, Appl. Phys. Lett. 103 (2013) (122106.
[10] Y. Oniki, H. Koumo, Y. Iwazaki, T. Ueno, J. Appl. Phys. 107 (2010) 124113.
[11] C.H. Lee, T. Tabata, T. Nishimura, K. Nagashio, K. Kita, A. Toriumi, Appl. Phys. Express 2 (2009) 071404.
[12] A. Yoshigoe, Y. Teraoka, R. Okada, Y. Yamada, M. Sasaki, J. Chem. Phys. 141 (2014) 174708.
[13] A. Yoshigoe, Y. Teraoka, Jpn. J. Appl. Phys. 49 (2010) 115704.
[14] D. Schmeisser, R.D. Schnell, A. Bogen, F.J. Himpsel, D. Rieger, G. Landgren, J. F. Morar, Surf. Sci. 172 (1986) 455.
[15] N. Tabet, M. Faiz, N.M. Handam, Z. Hussain, Surf. Sci. 523 (2003) 68.
[16] A. Molle, M.N.K. Bhuiyan, G. Tallarida, M. Fanciulli, Appl. Phys. Lett. 89 (2006) 083504.